Microchemical Journal 200 (2024) 110477

Contents lists available at ScienceDirect

Microchemical Journal

journal homepage: www.elsevier.com/locate/microc

Optimizing a radiochemical separation of ^{26}Al from an acidic V-rich matrix

Đorđe Cvjetinović [a,*], Xiaohan Pan [a,b], Jelena Petrović [a,c], Dorothea Schumann [a]

[a] Laboratory of Radiochemistry, Paul Scherrer Institut (PSI), Forschungsstrasse 111, 5232 Villigen, Switzerland
[b] School of Mechanical Engineering, Shanghai Jiao Tong University, Shanghai 200240, China
[c] Vinča Institute of Nuclear Sciences - National Institute of the Republic of Serbia, University of Belgrade, Mike Petrovića Alasa 12-14, 11351 Belgrade, Serbia

ARTICLE INFO

Keywords:
Aluminium
Vanadium
Extraction chromatography
Gamma spectroscopy
Non-carrier added

ABSTRACT

Sorption and desorption of Al(III) on a series of different extraction resins (LN, LN2, LN3, TK100, TK101, TK201) in acidic HNO_3 media containing high concentrations of V(IV,V) was investigated. Static batch studies were conducted as a way of obtaining preliminary distribution coefficient (K_d) values that were further used to develop dynamic tests on real samples. It was shown that a complete separation and recovery of Al(III) from V(V) under acidic conditions (pH = 2) is possible by utilizing LN resin. Active "hot" dynamic studies with ^{26}Al (≈10 Bq) as a radiotracer and real waste samples were conducted to further investigate and confirm the results of the inactive "cold" experiments. Utilizing this separation procedure, we have successfully removed all traces of ^{26}Al ($\sim 10^{-9}$ g) radiotracer from the bulk vanadium matrix.

1. Introduction

Within the Isotope and Target Chemistry (ITC) group at the Paul Scherrer Institute (PSI), different radiochemical procedures are developed in order to completely separate and purify individual radionuclides. Such procedures are developed either for ongoing irradiation experiments or for the post processing of waste produced in past experiments. Ideally, one would want to separate completely and individually each one of the valuable radionuclides present in the waste material [1]. Such waste recycling allows access to valuable radionuclides that can be used for completely new studies or at the very least as radiotracers [2]. When and if possible, a separation procedure is optimized in such a way that the radionuclide separation is done in a simple, straightforward way, preferably using a single adsorption chromatography column and without the use of a stable carrier so the maximum specific activity can be achieved.

During the SINCHRON project large amounts of waste were produced from which valuable radionuclides could be recovered (^{26}Al, ^{41,45}Ca, ^{44}Sc/^{44}Ti) in addition to the primary radionuclide of interest, ^{32}Si [1,2]. For this purpose, 150 vanadium discs (m ≈ 420 mg, purity 99.8 %, Goodfellow Cambridge Limited, U.K.) were irradiated for two years in the SINQ (the Swiss Spallation Source) Target Irradiation Program (STIP), using High-Intensity Proton Accelerator (HIPA, E^{p+}_{max} =590 MeV) [1,3]. Following the cooldown period that allowed the decay of short-lived radionuclides V-discs were dissolved and processed for ^{32}Si [1]. The residual solution waste was found to also contain several different exotic radionuclides that were of interest to recover as non-carrier added [2,4]. One of these valuable radionuclides was ^{26}Al and a non-carrier added ^{26}Al separation was developed and performed at ITC. Out of 150 V-discs 42 were processed for ^{26}Al and on average a specific activity of 5–10 Bq/g was obtained.

Development of a new and improved separation of ^{26}Al based on a single column adsorption/desorption step would be of great advantage. There are several reasons why, the main one being the simplification of the process since the waste samples are highly active due to the ^{60}Co presence and reduced operating time would minimize radiation exposure. Additionally, avoiding further waste inflation and producing higher specific activities of no-carrier added ^{26}Al would also be very beneficial for future experiments.

The importance of ^{26}Al extends across a multitude of scientific domains, from radiometric and cosmic ray exposure dating [5–7] to environmental tracing [8,9] and archaeological investigations [10–12]. Its role in radiotracer studies enables us to unravel aluminum's behavior in living organisms and track its movements in diverse materials. Moreover, in the domain of astrophysics [13–15], ^{26}Al contributes to our understanding of nucleosynthesis processes within stars and supernovae [16,17]. Meanwhile, in the field of environmental monitoring, it aids in resolving terrestrial processes [18], including sediment transport, soil erosion [19], and watershed dynamics [20].

Based on the remaining waste material (from 108 unprocessed V-

* Corresponding author.
E-mail address: djorde.cvjetinovic@psi.ch (Đ. Cvjetinović).

https://doi.org/10.1016/j.microc.2024.110477
Received 23 November 2023; Received in revised form 8 March 2024; Accepted 2 April 2024
Available online 3 April 2024

discs, 3M HNO_3) and previous studies performed at ITC it was decided to develop a new separation procedure that would allow for a straightforward recovery and preconcentration of ^{26}Al from V-rich waste samples [2,21]. For this purpose, an extensive study utilizing different extraction resins was performed on non-radioactive and radioactive samples in order to find optimal conditions at which a complete separation of Al from V would be possible. V is known to have different oxidation states (2+ to 5+) that result in the creation of different chemical species with varying properties which can lead to difficulties during separation [4,22–25]. Ideally, all of the ^{26}Al would be retained on the column, with the V showing no or minimal adsorption. This would allow us to run large volumes of radioactive solution with minimal human exposure and minimal waste inflation while also allowing us to elute a concentrated fraction of non-carrier added ^{26}Al in a single step.

Extraction resins LN, LN2, LN3, TK100, TK101, and TK201 from TrisKem (SAS, Bruz, France) were chosen for this study since they cover the optimal extraction range (from 2+ to 5+ oxidation states) for possible V and Al chemical species. The LN resins series was developed for specific lanthanide separation [26–29] and show affinity towards high oxidation states (3+ to 6+) while the main application of TK100/101/201 is for recovery of Sr, Pb, Ra, Cu, Tc, Rh [30–32] thus covering the 1+ to 7+ oxidation state range. These resins have different active groups as shown in Fig. 1.

2. Materials and methods

If not stated otherwise, all chemicals used in this study are commercially available and were purchased from Merck (KGaA, Germany) at p.a. purity and used without further purification. Solutions used for the experimental work were prepared volumetrically by diluting or dissolving commercial products using ultra-pure water (utp-H_2O, 18.2 MΩ cm, Veolia S.A.). Wherever possible, glassware was avoided and substituted with similar plastic products, such as polyethylene (PE), polymethyl methacrylate (PMMA), and polytetrafluoroethylene (PTFE). All of the different extraction resins were acquired from TrisKem (SAS, Bruz, France) and these include LN (20–50 μm), LN2 (20–50 μm), LN3 (20–50 μm), TK100 (100–150 μm), TK101 (100–150 μm), and TK201 (50–100 μm). Testing was done on both real and simulated samples, and a brief overview of their characteristics is given in Table 1.

2.1. Inductively coupled plasma – optical emission spectrometry (ICP-OES)

ICP-OES (Agilent 5110, Agilent Technologies, U.S.A.) was used to quantify the concentrations of Al and V in the cold studies (static and dynamic). Single-element standards (1000 mg/L, TraceCERT®, Merck KGaA, Germany) in various dilutions were used to prepare the appropriate measurement calibration curves. For these measurements, Al (396.152 nm), V (268.796 nm) and V (326.769 nm) optical emission lines were used (values for V are calculated as an average). These lines

Table 1
Real and simulated solutions of V/Al mix.

Solution	V	^{26}Al	Test	Origin	C_V [ppm]
S_0	4+	NO	Batch	Real	6500
S_1	4+	NO	Batch/Column	S_0	1250
S_2	5+	NO	Batch/Column	S_0	1250
S_3	5+	YES	Column	Real	3000–4000*
S_4	5+	YES	Column	S_0/S_3	4300–4500*

* *For active samples the concentration is estimated based on the dilution factor.*

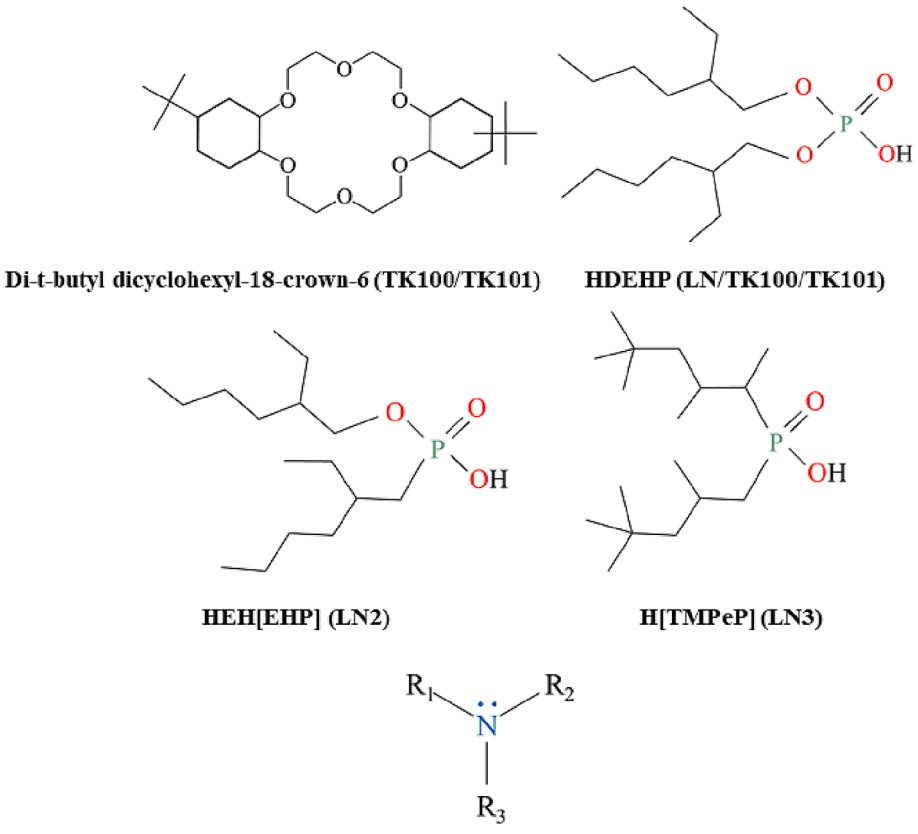

Fig.1. Active adsorption sites for LN, LN2, LN3, TK100, TK101 and TK201 resin.

were picked since they show the least amount of element cross-interference with a suitable emission intensity. Prior to the measurement all of the solutions were diluted 1:10 with freshly prepared 2 % HNO_3. Where applicable measurements were performed in triplicate with a triple emission acquisition per sample.

2.2. Distribution studies

Cold static studies were performed in a batch manner, briefly described as follows: pre-weighed amount of the corresponding resin (50 ± 2 mg) is transferred into a 2 ml vial; 0.5 ml of the appropriate solvent matrix is added to the vial; the vial is shaken for 30 min to precondition the resin; 1 ml of the appropriate Al/V standard solution of the same acidity/matrix is added to the vial; the vial is shaken overnight for 16h; vial is centrifuged at 15,000 rpm for 5 min; 0.5 ml of the supernatant is removed and transferred into a 15 ml vial; 4.5 ml of 2 % HNO_3 is added to the vial and the solution is vortexed for 3–5 s.

Samples prepared in such a way were then measured using ICP-OES and the concentration of both Al and V was determined. Maximum concentration was determined by making and measuring standard samples that were treated in the same way without the resin addition. From these measurements, the corresponding distribution coefficients (K_d) were calculated using the formula (1), shown as:

$$K_d = \frac{C_{max} - C_{mes}}{C_{mes}} \times \frac{V_{ml}}{m_g} \quad (1)$$

where C_{max} represents the maximum concentration of V/Al prior to resin contact (no adsorption); C_{mes} represents the concentration value of Al/V in the supernatant after contact with the resin (adsorption equilibrium); V_{ml} represents the solution volume in which the adsorption happened (1.5 ml); m_g is the mass of the resin added to the sample.

Initial distribution studies were done using ICP-OES standards for Al and V such that the concentration ratio was 1:10 (C_{Al} = 5 ppm: C_V = 50 ppm) in a wide acidity range. Subsequently the best performing resins were selected and retested in a narrower pH range with a real V-sample matrix (S_0) spiked with stable Al for both V(IV) and V(V) oxidation states (Table 1). In order to produce S_0 a single non-irradiated V-disc is treated as described previously [1] resulting in a 3M HNO_3 V-rich solution. The initial V concentration of S_0 is $C_V \approx 6500$ ppm before Al spiking, dilution and oxidation in order to create samples S_1 and S_2. Sample S_0 was first diluted and then spiked with Al so the rough ratio between C_V and C_{Al} was 1:10 in samples S_1 and S_2, as in initial distribution measurements.

As shown before and indicated by the blue color of the S_0 the dominant form of V in the S_0 is V(IV) in the form of VO^{2+} ion [1,4]. For samples S_1 and S_2 the pH value was adjusted to pH ≈ 2, first by using solid NaOH followed by a fine pH adjustment using a freshly prepared 5M NaOH solution. Addition of solid NaOH was performed in increments while the sample vessel was submerged in an ice bath. Fine adjusting using a 5M NaOH solution was done while the sample was magnetically stirred. Additionally, sample S_2 was prepared by oxidizing S_0 with a fresh batch of conc·H_2O_2 (easily observable chromatic transition from blue to yellow). Following the oxidation process, sample S_2 was heated at 60 °C for 1h and left overnight in a stream of N_2 in order to decompose the remaining H_2O_2 and remove residual gas bubbles. Resins that showed the best K_d ratio ($>10^2$) for separation of Al from V under these conditions were further selected and tested in dynamic conditions. Both V(V) and V(IV) oxidation states were tested, and the appropriate elution curves were obtained. For elution curve studies samples S_1 (V(IV) dominant form) and S_2 (V(V) dominant form) were prepared from S_0 by Al spiking to reach an approximate C_{Al}/C_V ratio of 1:100.

2.3. Column tests

Custom made PMMA columns (length = 100/200 mm, inner diameter = 10 mm) were used for the column setup utilized in elution curve studies and hot active-sample studies. Columns loaded with the appropriate resin height of 40/120 mm and a flow rate of f = 1.5 ml/min were used for all the runs. Peristaltic pumps (REGLO Digital MS-2/8, Cole-Parmer Instrument Company, LLC., U.S.A.) were used for the separations, with the same squeeze tubes (Ismaprene PharMed®, SC0307, Cole-Parmer Instrument Company, LLC., U.S.A.). Resin inside the column was immobilized with two (bottom-top) PE frits (inner diameter = 10 mm, 10 μm pore-size, Kinesis Group from Cole-Parmer Instrument Company, LLC., U.S.A.).

Typical pretreatment of the resin involves rinsing the resin (3×) with utp-H_2O, leaving it to settle and decanting it, followed by the addition of a 3 % ethanol solution and storage for 24h. The resin is then loaded and settled in the column. Subsequently, the column is washed with utp-H_2O (100 ml), followed by 0.01M HNO_3 (100 ml) at the flow rate of f = 1.5 ml/min, and left to settle for 4h. Prior to use, the column is pre-washed with another 50 ml of 0.01M HNO_3.

A column run is divided into three steps differentiated by the addition of different fractions: (1) Load fraction (L) represents the initial solution from which the desired element(s) need to be separated by sorbing/desorbing at the stationary phase; (2) Wash fraction (W) that matches the solution matrix of the load fraction without the elements being sorbed/desorbed, with the purpose of washing away any free non-adsorbed elements; (3) Elution fraction (E) serves to desorb the wanted element(s) in such a way that minimal or no postprocessing and purification is needed.

In the case of obtaining the elution curves for non-active cold solutions of Al(III)/V(IV) (S_1) and Al(III)/V(V) (S_2) all three fractions (L, W, E) are volumetrically equivalent (20 ml). Wash fraction is 0.01M HNO_3 while the elution fraction is 3M HNO_3. During a column run (resin height = 40 mm) fractions are loaded onto the column in the order of L/W/E and every 2 ml are collected separately in order to construct the appropriate elution curve. From these 2 ml a fraction of 0.5 ml is removed and diluted with 4.5 ml of 2 % HNO_3 before being measured using ICP-OES, in the manner previously described. The approximate concentration ratio between C_{Al}/C_V before a column run was 1:100.

Besides non-active cold column runs active hot column runs are also performed in an analogue way, by using different volumes for L/W/E fractions. In the case of a real waste sample (S_3) fraction volumes are L = 200 ml / W = 50 ml / E = 30 ml (resin height = 120 mm) while for the cold V-matrix spiked with ^{26}Al (≈10Bq) sample (S_4) fraction volumes are L = 300 ml / W = 50 ml / E = 40 ml (resin height = 120 mm).

A final purification step of the ^{26}Al is done by utilizing an anion-exchange step described previously [2]. In short, 10 ml of S_4 elute is evaporated down to dryness on a PTFE evaporation dish and collected in 50 ml of 0.1M HF. This solution is then used as a load on an anion-exchange column that is prepared by using Dowex®1X8 resin (200–400 mesh, Sigma-Aldrich, Germany). Column height is set to 40 mm with a flow rate at 1.5 ml/min. Anion-exchange resin is rinsed with H_2O (3×) and left for 24h to settle before loading the column and leaving it to settle. Prior to use column is washed with utp-H_2O (100 ml) followed by preconditioning with 0.1M HF (100 ml) and left to settle for 4h. The column is then loaded with the 50 ml of 0.1M HF solution containing ^{26}Al, followed by a 10 ml 0.1M HF wash step and then finally an elution step using a 1M HCl.

2.4. Gamma spectroscopy

Elute fractions obtained during column runs of real waste and simulated ^{26}Al/V samples (S_3-S_4) were measured using an HPGe high resolution gamma detector (Mirion Technologies, California, U.S.A.) for 24h. To verify and quantify the ^{26}Al recovery yield for the proposed separation the elution fraction from S_3 was used to spike an inactive V-matrix solution (S_0) in order to prepare a simulated ^{26}Al/V sample (S_4). For all the measurements a relatively low background gamma detector setup was used with the appropriate background acquisition. The presence of ^{26}Al is easily observed via detection of the 1808.65(7) keV

gamma line. It was not possible to measure the real waste sample S_3 for ^{26}Al prior to column separation with the same gamma detector setup. This is due to the high activity coming from ^{60}Co present in the waste sample S_3. Using a different gamma detector setup, it was possible to measure the S_3 sample but no ^{26}Al was detected (data not shown), as was expected due to the high ^{60}Co activity and an unfavorable geometry, since the activity of ^{26}Al was estimated to be approximately $\leq$10 Bq.

3. Results and discussion

Results obtained in the preliminary distribution study, shown in Table 2. indicate that the resin LN might be the best candidate for separating Al from V. Extremely high K_d(Al) value (>37000) at 0.01M HNO_3 indicates strong sorption in contrast to the K_d(V). As for LN2 and LN3 they seem to show much less preference to Al for all points in comparison to LN. Based on the data from Table 2. resin LN3 was excluded from any further analysis since the K_d values are not in the optimal range. Under different circumstances LN2 might be considered as a separation tool at 0.01M HNO_3 however there is a large gap between the corresponding K_d values for both Al and V in comparison to LN. Considering that LN resin was specifically designed to separate lanthanides it should be no surprise that it shows high affinity for Al^{3+} as well. Adsorption properties of LN increase with the oxidation state of the element (from 3+ to 6+) explaining the affinity toward Al^{3+}. In the case of V there are different chemical species present depending on the oxidation state such as VO^{2+} or VO_2^+ that show lower affinity towards the LN resin, as is expected for 1+ and 2+ species.

While LN in general has shown the best distinction between Al and V sorption under these conditions, the TK type resins also must be considered. Overall, they show low affinity towards both Al and V, except for TK100 and TK201 at 0.01M HNO_3. Similarly, to LN and LN2, TK100 shows good adsorption of Al for 0.01M HNO_3, though the K_d ratios are much less in its favor. In the case of the TK101 it seems that neither element can be properly adsorbed, and this resin was disregarded from further testing. Interestingly, the TK201 shows no Al adsorption over the entire tested range while it exhibits moderately high K_d values for V at 0.01M HNO_3.

These preliminary studies were conducted using V and Al standards and therefore both V(V) and V(IV) are presumed to be present in the solution mix (non-oxidation state adjusted). The reason to perform this study was in case that we simultaneously have V(IV) and V(V) species in our real sample. Vanadium can form a large and different variety of cationic, anionic, neutral, dimeric and polymeric species depending on the solution pH, oxidation states present and the V concentration itself [22–25,33]. Under the experimental conditions in our study, we can presume that the dominant species are VO_2^+ and VO^{2+}, depending on the V oxidation state. Additionally, it is also possible to have traces of H_3VO_4, $H_2VO_4^-$ and $H_3V_2O_7^-$ as well [22–25,33]. Because this can lead to false interpretation these initial results only served to point out the best resin candidates for oxidation-controlled studies.

As both LN and TK201 resins have the highest affinity towards a single element from the mix further tests were conducted on the S_1 and S_2 samples. Results of these tests are shown in Tables 3–4, and it is presumed that in these cases the oxidation state of V is controlled (either IV or V). For LN resin it seems that the K_d values of both Al(III) and V(IV) increase as the acidity drops and are relatively high, as seen in Table 3. The changes in K_d values of both elements are drastic and can again be attributed to the change in V oxidation state, going from a mix of V(IV)/V(V) to a dominant V(IV) oxidation state. For 0.01M it is shown that Al is now completely sorbed which is comparable to the results presented in Table 2. Keeping in mind that these measurements were done on a simulated S_1 sample, with a concentration ratio of 1:10 in favor of V, it is safe to say that LN at these conditions seems to be much more preferential for Al than for V.

A lack of Al adsorption is again observed for TK201, as was the case in the previous tests, and this time the adsorption of V seems to change as well (Table 3). The change is not too drastic and is expected since the sample matrix was changed with V(IV) being the dominant oxidation state. Still the relatively high K_d(V) value at 0.01M (>400) indicates that it might be worthwhile to test the separation at these conditions. Possibly no Al would be absorbed while V would remain on the column. In this case Al would remain in the load and wash fraction, meaning no elution would be needed to recover Al. This also means that Al would be dispersed in a relatively large volume (larger than at start) implying the need for further processing. Additionally, such a column would require larger amounts of TK201 resin that are capable of adsorbing macroscopic amounts of V. Because of these reasons the complete V/Al separation even, if possible, would not be optimal.

Nevertheless, fast column tests were performed with LN (0.01–0.1M) and TK201 (0.01M). The idea was to quickly and visually (adsorption of the blue VO^{2+} ion on the column) identify possible conditions at which Al could be separated. These visual tests showed that VO^{2+} is not completely absorbed with TK201 (0.01M), as seen by the residual

Table 2
K_d values for Al(III) and V(IV)/V(V) mix in HNO_3.

Resin	C(HNO_3) [M]	K_d (Al) [ml/g]	K_d (V) [ml/g]
LN	0.010	37900 ± 2800	24.3 ± 1.3
	0.100	123 ± 6	3.78 ± 0.19
	1.000	min. ads. *	min. ads.
	3.000	min. ads.	min. ads.
LN2	0.010	1814 ± 91	92.6 ± 4.7
	0.100	9.09 ± 0.45	3.46 ± 0.17
	1.000	min. ads.	min. ads.
	3.000	min. ads.	min. ads.
LN3	0.010	4.46 ± 0.22	64.7 ± 3.3
	0.100	min. ads	2.20 ± 0.11
	1.000	min. ads.	min. ads.
	3.000	min. ads.	min. ads.
TK100	0.010	348 ± 17	3.64 ± 0.18
	0.100	4.10 ± 0.21	0.98 ± 0.05
	1.000	min. ads.	0.77 ± 0.05
	3.000	min. ads.	0.52 ± 0.03
TK101	0.010	min. ads.	min. ads.
	0.100	min. ads.	0.23 ± 0.03
	1.000	min. ads.	min. ads.
	3.000	4.58 ± 0.23	8.79 ± 0.44
TK201	0.010	min. ads.	414 ± 22
	0.100	min. ads.	1.04 ± 0.05
	1.000	min. ads.	0.72 ± 0.04
	3.000	min. ads.	min. ads.

* min.ads. means that element concentration is unchanged in the supernatant indicating that there is no adsorption.

Table 3
K_d values for Al(III) and V(IV) in a simulated V/Al sample.

Resin	C(HNO_3) [M]	K_d(Al)[ml/g]	K_d(V)[ml/g]
TK201	0.010	0.36 ± 0.02	454 ± 23
	0.025	min. ads.	73.3 ± 4.3
	0.050	min. ads.	0.85 ± 0.04
	0.100	0.36 ± 0.02	0.96 ± 0.05
LN	0.010	max. ads. **	2000 ± 100
	0.025	1902 ± 96	405 ± 21
	0.050	938 ± 48	111.9 ± 5.6
	0.100	194.2 ± 9.8	30.4 ± 1.6

*min.ads. means that element concentration is unchanged in the supernatant indicating that there is no adsorption.

**max.ads. means that no element was detected in the supernatant indicating maximum adsorption.

Table 4
K_d values for Al(III) and V(V) in a simulated V/Al sample.

Resin	C(HNO_3) [M]	K_d(Al)[ml/g]	K_d(V)[ml/g]
TK201	0.010	min. ads.*	min. ads.
	0.025	min. ads.	min. ads.
	0.050	min. ads.	min. ads.
	0.100	min. ads.	min. ads.
LN	0.010	1816 ± 91	min. ads.
	0.025	1102 ± 55	0.58 ± 0.03
	0.050	740 ± 37	min. ads.
	0.100	357 ± 18	min. ads

*min.ads. means that element concentration is unchanged in the supernatant indicating that there is no adsorption.
**max.ads. means that no element was detected in the supernatant indicating maximum adsorption.

coloring of the load fraction after passing through the column. While for LN, it was confirmed that VO^{2+} adsorption decreases as the acidity drops (data not shown). However, VO^{2+} adsorption is still clearly visible on the LN column at 0.1M HNO_3. Based on these visual tests it was decided to try to adsorb both Al and V with an LN column from the 0.01M HNO_3 matrix, and then wash out V with 0.01M HNO_3, followed by Al elution with 3M HNO_3. To test this hypothesis the elution behavior (Fig. 2) was studied using a simulated cold S_1 V(IV) containing sample spiked with Al.

Distribution studies conducted on sample S_2 that has V(V) oxidation state are shown in Table 4. and they clearly indicate that TK201 cannot adsorb either Al or V from the mix. For LN we can observe a different behavior, where no V is adsorbed across the tested pH range, while Al seems to adsorb well, especially for 0.01M HNO_3 matrix. It is important to note that K_d(Al) is higher in the case of V(IV) being the dominant oxidation state (Table 3.) though we also observe a relatively high adsorption of V. In the case of trace amounts of Al compared to high content of V, this can be a limiting factor to perform a successful separation due to competition between ions.

Data shown in Fig. 2 indicates it's impossible to have a complete V/Al separation using the proposed conditions. To the contrary of what was expected, most of the Al is not sorbed and there is a breakthrough. In the best-case scenario, it would be possible to recover approximately 48 % of Al without V contamination, by collecting the initial part of the load fraction. At the same time around 68 % of V is retained on the column and easily eluted with 3M HNO_3, however, this V fraction is not Al free. Such behavior could possibly be explained by the concentration ratio between Al and V in the simulated sample, where V(IV) simply overwhelms the column and the corresponding adsorption sites, making them inaccessible to Al.

Results shown in Table 3. as well as the literature data [21] indicate that it should be possible to strongly adsorb Al^{3+} with the LN resin at pH = 2, yet the high V(IV) content seems to be the problem, as it readily adsorbs as well. This can be deduced by the large change in adsorption of V compared to the tests done with V(IV)/V(V) mix and just V(IV). Because of this and the results shown in Table 4. another elution curve was tested, this time using sample S_2 and V(V) oxidation state (Fig. 3). By changing the oxidation state of V using conc·H_2O_2, it might be possible to reduce the affinity of LN towards the resulting V species as indicated by distribution studies (Table 4.). As presumed, the change in V oxidation state brought significantly better results in terms of Al/V column separation, as seen in Fig. 3. A complete separation between Al (III) and V(V) seems to be achievable under these conditions. Seemingly no VO_2^+ is retained on the column during the loading phase, while Al^{3+} is completely eluted with 3M HNO_3.

The adsorption behavior of Al and V on LN columns shown in Fig. 2 and Fig. 3 can perhaps be explained by the presence of different V species and the extraction method LN resin is based on. As mentioned previously LN resin is a cationic extraction resin, most commonly used for lanthanide separation or in general for trivalent metal ions (M^{3+}) [29]. The extraction mechanism can be represented by equation (2):

$$M^{3+} + \overline{3(HY)_2} \rightleftharpoons 3H^+ + \overline{M(HY_2)_3} \quad (2)$$

The efficiency of this extraction mechanism will change significantly with the charge of the species and as the charge decreases so will the efficiency of extraction. As seen in Fig. 2 it seems that V(IV) is only partially adsorbed by LN, while it is constantly being washed away by the 0.01M HNO_3, indicating a weak adsorption. In the case of V(V) we see that no adsorption is observable (Fig. 3), and this seems to confirm that the dominant V species in S_1 and S_2 are VO^{2+} and VO_2^+, as expected. It is important to note that it is possible that traces of other V(V) species are present in S_2, such as H_3VO_4, $H_2VO_4^-$ and $H_3V_2O_7^-$. Even if this is the case, these species are not cationic, and they will not interfere with the separation since they cannot be adsorbed by LN under these conditions.

Based on the results obtained with the model inactive solutions the same separation procedure was applied to a real system using active samples S_3 and S_4. Following the column separation of sample S_3 it is clear that ^{26}Al is detected in the elute phase, as can be seen in the gamma spectra of the elute S_3 shown in Fig. 4. The 1809 keV line of ^{26}Al is readily visible, indicating that Al can be recovered under these conditions, even when present in extremely low concentrations. Besides ^{26}Al

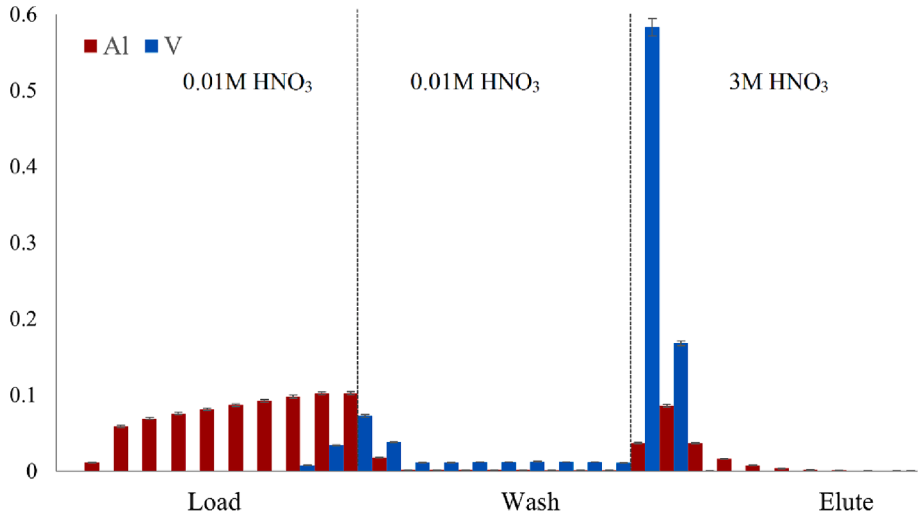

Fig.2. Elution curve of an Al(III)/V(IV) solution on LN resin (f = 1.5 ml/min, H = 40 mm, M_{tot}(V) ≈ 25 mg).

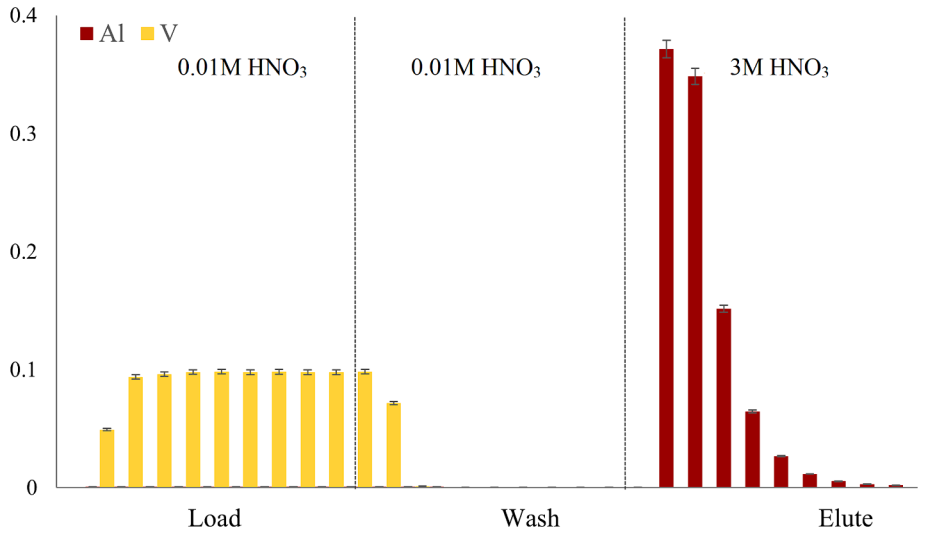

Fig.3. Elution curve of an Al(III)/V(V) solution on LN resin (f = 1.5 ml/min, H = 40 mm, $M_{tot}(V) \approx 25$ mg).

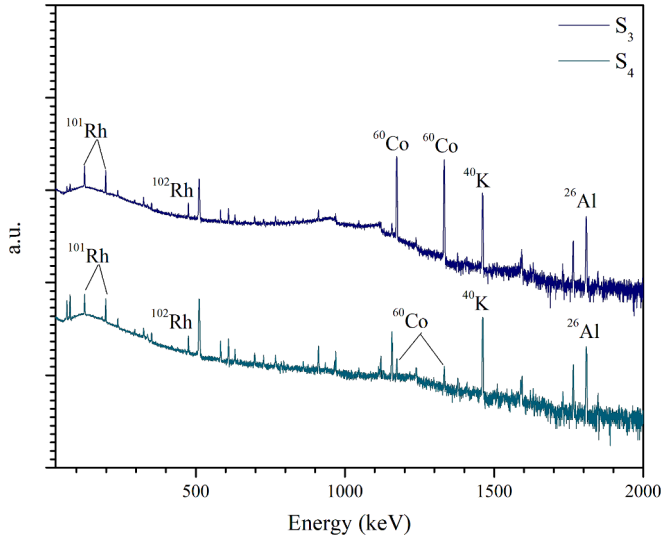

Fig.4. The 24 h γ-spectra of ^{26}Al in elutes of samples S_3 (top) and S_4 (bottom).

some other radionuclides are detected in trace amounts, such as ^{60}Co, ^{101}Rh, ^{102,102m}Rh. Prior to the column separation sample had a relatively high dose rate on contact (5–10 mSv/h), due to the large ^{60}Co activity present in S_3. After the separation, the elute had a slightly above the background dose rate (8–12 μSv/h) indicating that most of the ^{60}Co was not retained on the column.

Additionally, the column separation of sample S_4 allows for easy quantification of ^{26}Al recovery, since the elute from S_3 was used to spike a cold V-matrix with a known activity of ^{26}Al in order to create sample S_4. Quantification of activity was done under the same conditions, including using the same geometry, and the results were normalized. By comparing the activities for S_3 vs. S_4 elutes it was found that the ^{26}Al recovery is 98.2 ± 4.1 %. Additionally, the activity of ^{101}Rh present in the elutes was also compared between S_3 and S_4, showing excellent agreement of 97.9 ± 4.8 % (for 127.6 keV gamma line) and 103.7 ± 4.1 % (for 198 keV gamma line). This was done to further confirm the results for ^{26}Al recovery yield, since the overall low activity of ^{26}Al can lead to a higher uncertainty prediction. As expected, the activity of detectable ^{60}Co decreased significantly (~10^2) which is in good agreement with the data for S_3 prior to and following column separation. These results, obtained in both cold and hot experiments, indicate that it is possible to achieve a complete separation of Al(III) from V(V) under acidic conditions.

As seen from the gamma spectra of the final solution in Fig. 5 it is obvious that the ^{101,102}Rh radionuclides were successfully removed from the S_4 elute utilizing an additional anion exchange step. With this final step being successful, we developed a new and optimized scheme for ^{26}Al separation and purification (Fig. 6a) compared to the procedure used previously (Fig. 6b). A simple visual comparison between the separation schemes shown in Fig. 6 indicates that the process has been significantly simplified. Also, the volume of material that can be processed in a continuous single step has been increased from 1 to 10 V-disc fractions. The final anion-exchange step in the optimized separation scheme is only required if radionuclides of Rh are detected in the solution. In this case, just a single evaporation/anion-exchange step is needed to completely purify the fraction from ^{101,102}Rh and any traces of ^{54}Mn and ^{60}Co that might remain after the LN separation. Adjusted for volumes, specific activities of resulting ^{26}Al solutions can be 2 to 3 times higher than before, up to 30 Bq/g which is a significant increase.

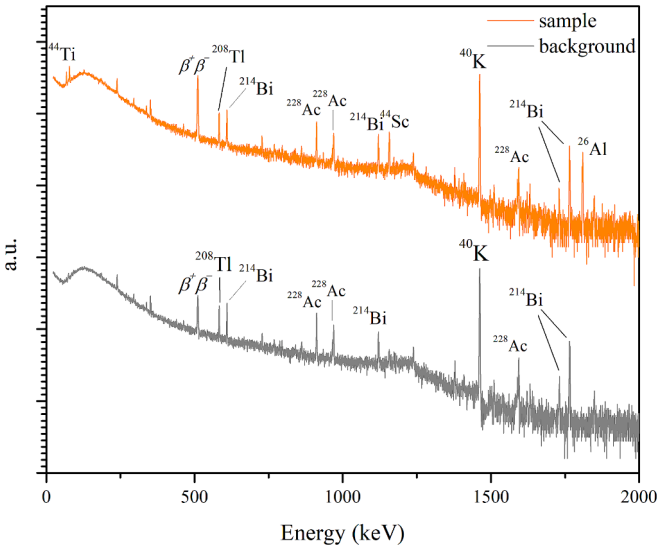

Fig.5. The 24 h γ-spectra of final ^{26}Al sample (top) and background (bottom).

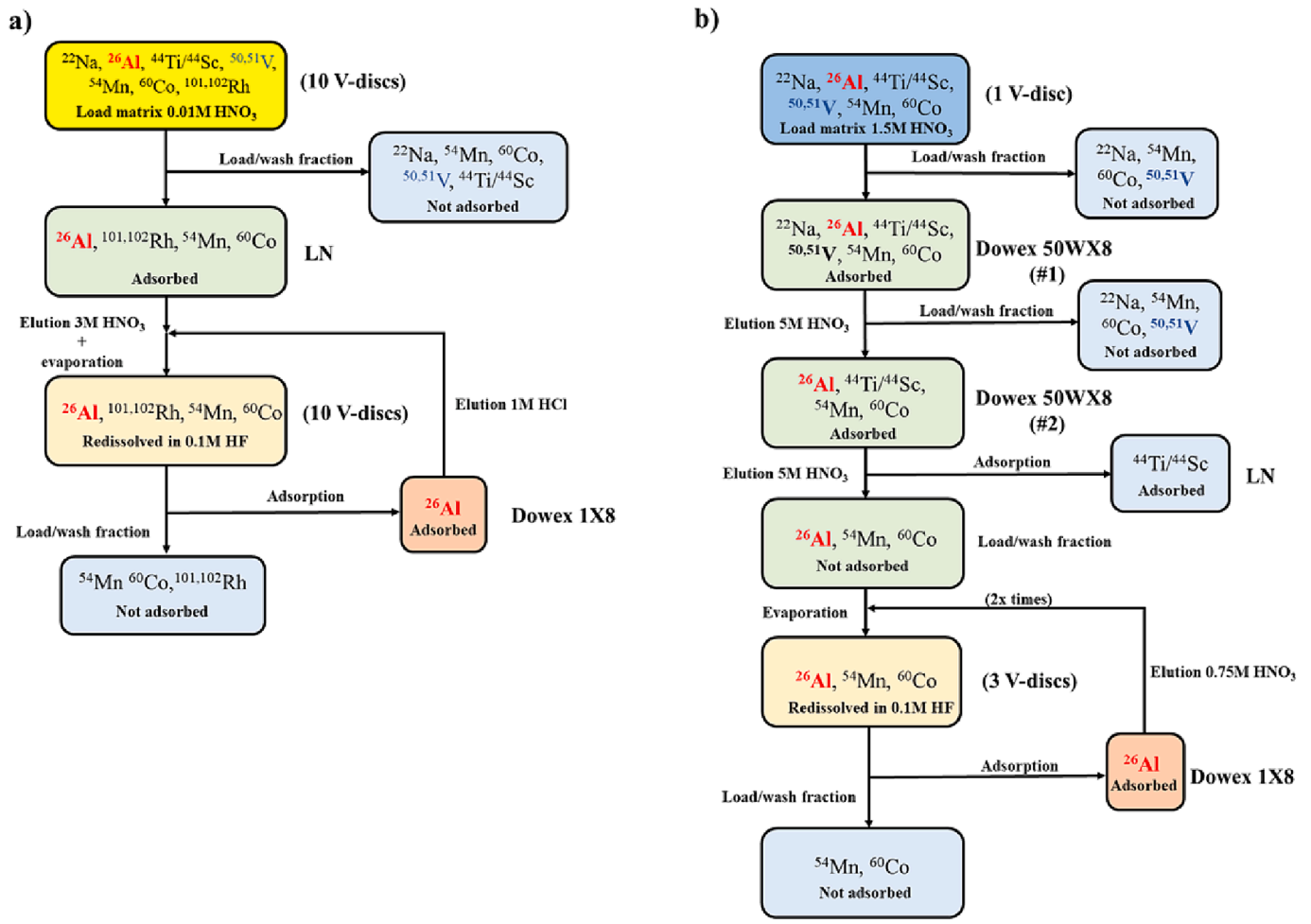

Fig.6. Optimized a) and previously developed b) radiochemical separation scheme of ^{26}Al.

4. Conclusion

In this study, we systematically investigated the efficacy of various extraction resins to achieve a complete separation of aluminum (Al) from a vanadium (V) matrix. Through a series of designed experiments, including both cold and hot tests, we have demonstrated that the LN resin stands out as the optimal choice for this purpose. Our findings highlight the significance of specific conditions in achieving this significant separation, with a critical emphasis on the need for the complete oxidation of V to V(V) state that leads to the formation of VO_2^+ species. This critical parameter plays an essential role in ensuring the success of the procedure. It allows for a direct, one-step separation of Al from V, presenting a highly efficient method that can be readily applied for the recovery of valuable Al radionuclides and the purification of vanadium.

Research funding

This project is funded by the Swiss National Science Foundation (SNSF) as part of SINERGIA (No. 177229) and receives additional financial support from the European Union's Horizon 2020 research and innovation program under the Marie Skłodowska-Curie grant agreement No. 884104 (PSI-FELLOW-III-3i).

CRediT authorship contribution statement

Đorđe Cvjetinović: Writing – original draft, Validation, Methodology, Formal analysis, Data curation, Conceptualization. **Pan Xiaohan:** . **Jelena Petrović:** Writing – original draft, Validation, Investigation, Formal analysis. **Dorothea Schumann:** Writing – review & editing, Project administration, Funding acquisition, Data curation.

Declaration of competing interest

The authors declare that they have no known competing financial interests or personal relationships that could have appeared to influence the work reported in this paper.

Data availability

Data will be made available on request.

References

[1] M. Veicht, I. Mihalcea, Đ. Cvjetinovic, D. Schumann, Radiochemical separation and purification of non-carrier-added silicon-32, Radiochim. Acta. 109 (2021) 735–741, https://doi.org/10.1515/ract-2021-1070.
[2] J.M. Wilson, I. Mihalcea, M. Veicht, Đ. Cvjetinović, D. Schumann, Recovery of no-carrier-added 41 Ca, 44 Ti, and 26 Al from high-energy proton-irradiated vanadium targets, Radiochim. Acta. 111 (2023) 265–271, https://doi.org/10.1515/ract-2022-0072.
[3] Y. Dai, G. Bauer, Status of the first SINQ irradiation experiment, STIP-I, J. Nucl. Mater. 296 (2001) 43–53, https://doi.org/10.1016/S0022-3115(01)00544-X.
[4] M. Veicht, I. Mihalcea, P. Gautschi, C. Vockenhuber, S. Maxeiner, J.C. David, S. Chen, D. Schumann, Radiochemical separation of 26Al and 41Ca from proton-irradiated vanadium targets for cross-section determination by means of AMS, Radiochim. Acta. 110 (2022) 809–816, https://doi.org/10.1515/ract-2022-0036.
[5] Y. Yokoyama, M. Yamane, A. Nakamura, Y. Miyairi, K. Horiuchi, T. Aze, H. Matsuzaki, Y. Shirahama, Y. Ando, In-situ and meteoric 10Be and 26Al measurements: Improved preparation and application at the University of Tokyo,

Nucl. Instruments Methods Phys. Res. Sect. B Beam Interact. with Mater. Atoms. 455 (2019) 260–264. https://doi.org/10.1016/j.nimb.2019.01.026.
[6] G.K. Atsunori Nakamura, Y. Yokoyama, Y. Sekine, K. Goto, T.M.P. Senthil Kumar, Hiroyuki matsuzaki, ichiro kaneoka, formation and geomorphologic history of the Lonar impact crater deduced from in situ cosmogenic 10Be and 26Al, geochemistry, Geophys. Geosystems. 15 (2014) 4692–4711, https://doi.org/10.1002/2014GC005376.Received.
[7] T. Fujioka, D. Fink, C. Mifsud, Towards improvement of aluminium assay in quartz for in situ cosmogenic 26Al analysis at ANSTO, Nucl. Instruments Methods Phys. Res. Sect. B Beam Interact. with Mater. Atoms. 361 (2015) 346–353, https://doi.org/10.1016/j.nimb.2015.07.120.
[8] K. Kretschmer, R. Diehl, M. Krause, A. Burkert, K. Fierlinger, O. Gerhard, J. Greiner, W. Wang, Kinematics of massive star ejecta in the milky way as traced by 26Al, Astron. Astrophys. Rev. 559 (2013) 1–11, https://doi.org/10.1051/0004-6361/201322563.
[9] L.A. Perg, R.S. Anderson, R.C. Finkel, Use of a new 10Be and 26Al inventory method to date marine terraces, Santa Cruz, California, USA, Geology. 29 (2001) 879–882, https://doi.org/10.1130/0091-7613(2001)029<0879:UOANBA>2.0.CO;2.
[10] B.A. Hofmann, S.B. Schreyer, S. Biswas, L. Gerchow, D. Wiebe, M. Schumann, S. Lindemann, D.R. García, P. Lanari, F. Gfeller, C. Vigo, D. Das, F. Hotz, K. von Schoeler, K. Ninomiya, M. Niikura, N. Ritjoho, A. Amato, An arrowhead made of meteoritic iron from the late bronze age settlement of mörigen, Switzerland and its possible source, J. Archaeol. Sci. 157 (2023) 105827, https://doi.org/10.1016/j.jas.2023.105827.
[11] F. Han, J.J. Bahain, P. Voinchet, M. Jin, G. Yin, Radiometric dating of meipu hominin site in China by coupled ESR/U-series and cosmogenic 26Al/10Be burial dating methods, Quat. Geochronol. 70 (2022) 101295, https://doi.org/10.1016/j.quageo.2022.101295.
[12] G. Siron, K. Fukuda, M. Kimura, N.T. Kita, High precision 26Al-26Mg chronology of chondrules in unequilibrated ordinary chondrites: evidence for restricted formation ages, Geochim. Cosmochim. Acta. 324 (2022) 312–345, https://doi.org/10.1016/j.gca.2022.02.010.
[13] R. Diehl, H. Halloin, K. Kretschmer, G.G. Lichti, V. Schönfelder, A.W. Strong, A. von Kienlin, W. Wang, P. Jean, J. Knödlseder, J.-P. Roques, G. Weidenspointner, S. Schanne, D.H. Hartmann, C. Winkler, C. Wunderer, Radioactive 26Al from massive stars in the Galaxy, Nature. 439 (2006) 45–47, https://doi.org/10.1038/nature04364.
[14] R. Dressler, M. Ayranov, D. Bemmerer, M. Bunka, Y. Dai, C. Lederer, J. Fallis, A. Stj Murphy, M. Pignatari, D. Schumann, T. Stora, T. Stowasser, F.K. Thielemann, P.J. Woods, 44Ti, 26Al and 53Mn samples for nuclear astrophysics: The needs, the possibilities and the sources, J. Phys. G Nucl. Part. Phys. 39 (2012). https://doi.org/10.1088/0954-3899/39/10/105201.
[15] A.M. Laird, M. Lugaro, A. Kankainen, P. Adsley, D.W. Bardayan, H.E. Brinkman, B. Côté, C.M. Deibel, R. Diehl, F. Hammache, J.W. den Hartogh, J. José, D. Kurtulgil, C. Lederer-Woods, G. Lotay, G. Meynet, S. Palmerini, M. Pignatari, R. Reifarth, N. de Séréville, A. Sieverding, R.J. Stancliffe, T.C.L. Trueman, T. Lawson, J.S. Vink, C. Massimi, A. Mengoni, Progress on nuclear reaction rates affecting the stellar production of 26Al, J. Phys. G Nucl. Part. Phys. 50 (2023), https://doi.org/10.1088/1361-6471/ac9cf8.
[16] R. Diehl, A.J. Korn, B. Leibundgut, M. Lugaro, A. Wallner, Cosmic nucleosynthesis: a multi-messenger challenge, Prog. Part. Nucl. Phys. 127 (2022) 103983, https://doi.org/10.1016/j.ppnp.2022.103983.
[17] F. Hammache, D. Beaumel, S. Franchoo, I. Matea, P. Roussel, D. Suzuki, I. Stefan, A. Coc, J. Duprat, C. Hamadache, J. Kiener, V. Tatischeff, A.M. Laird, S.P. Fox, B.R. Fulton, C.A. Diget, J. Riley, F. De Oliveira, B. Bastin, Destruction of 26 Al in massive stars : study of the Al (n , p) 26 Mg and 26 Al (n , α) 23 Na reactions through the, 2444 (2023) 1–5.
[18] Z. Tymiński, M. Hult, A.M. Krzesińska, K. Tymińska, G. Lutter, P. Saganowski, G. Marissens, H. Stroh, A. Burakowska, T. Ziemek, M. Stachowicz, A. El-Mallul, Underground radioactivity measurements of meteorites: development of methods suitable to determine precise terrestrial age of recent falls, Appl. Radiat. Isot. 195 (2023), https://doi.org/10.1016/j.apradiso.2023.110733.
[19] Z. Xiaolong, X.U. Sheng, C.U.I. Lifeng, Z. Maoliang, Z. Zhiqi, Erosions on the Southern Tibetan Plateau 32 (2022) 333–357.
[20] E.M. Clapp, P.R. Bierman, A.P. Schick, J. Lekach, Y. Enzel, M. Caffee, Sediment yield exceeds sediment production in arid region drainage basins, Geology. 28 (2000) 995–998. https://doi.org/10.1130/0091-7613(2000)28<995:SYESPI>2.0.CO;2.
[21] S.H.D. Schumann, The purification of 26Al and 179TA recovered from irradiated steels of the SINQ target irradiation program, Annu. Rep. 2018 (266) (2018) 32–33.
[22] K. Pyrzyska, Determination of vanadium species in environmental samples, Talanta. 64 (2004) 823–829, https://doi.org/10.1016/j.talanta.2004.05.007.
[23] I. Boukhobza, D.C. Crans, Application of HPLC to measure vanadium in environmental, biological and clinical matrices, Arab. J. Chem. 13 (2020) 1198–1228, https://doi.org/10.1016/j.arabjc.2017.10.003.
[24] R. Zhang, J. Lu, M. Dopson, T. Leiviskä, Vanadium removal from mining ditch water using commercial iron products and ferric groundwater treatment residual-based materials, Chemosphere. 286 (2022) 131817, https://doi.org/10.1016/j.chemosphere.2021.131817.
[25] K. Kustin, Aqueous vanadium ion dynamics relevant to bioinorganic chemistry: a review, J. Inorg. Biochem. 147 (2015) 32–38, https://doi.org/10.1016/j.jinorgbio.2014.12.009.
[26] D.R. McAlister, E.P. Horwitz, Characterization of Extraction of chromatographic materials containing Bis(2-ethyl-1-hexyl)phosphoric acid, 2-Ethyl-1-hexyl (2-Ethyl-1-hexyl) phosphonic acid, and Bis(2,4,4-Trimethyl-1-pentyl)phosphinic acid, Solvent Extr. Ion Exch. 25 (2007) 757–769, https://doi.org/10.1080/07366290701634594.
[27] E.P. Horwitz, C.A.A. Bloomquist, Chemical separations for super-heavy element searches in irradiated uranium targets, J. Inorg. Nucl. Chem. 37 (1975) 425–434, https://doi.org/10.1016/0022-1902(75)80350-2.
[28] E.P. Horwitz, D.R. McAlister, A.H. Bond, R.E. Barrans, J.M. Williamson, A process for the separation of 177Lu from neutron irradiated 176Yb targets, Appl. Radiat. Isot. 63 (2005) 23–36, https://doi.org/10.1016/j.apradiso.2005.02.005.
[29] T.I.P.S.L./ L./ L. Resins, LN / LN2 / LN3 resins, 33 (2020). https://www.triskem-international.com/scripts/files/5f46343a7c97d9.45835022/PS_LN-Resin_EN_200603.pdf.
[30] Triskem International Product Sheet TK100/TK101 resins, TK100 / TK101 Resins, 33 (2023). https://www.triskem-international.com/scripts/files/63e0f4b439ea20.61110765/PS_TK101-Resin_EN_230206.pdf.
[31] Triskem International Product Sheet TK201 resins, TK201 resin, 33 (2022) 5–8. https://www.triskem-international.com/scripts/files/624a3ab0aba5d6.17415344/PS_TK201-Resin_EN_220330.pdf.
[32] D. Read, C.D.S. Happel, The behaviour of 226 Ra in high-volume environmental water samples on TK100 resin, (2017) 105–110. https://doi.org/10.1007/s10967-017-5203-4.
[33] G. Oriji, Y. Katayama, T. Miura, Investigation on V(IV)/V(V) species in a vanadium redox flow battery, Electrochim. Acta. 49 (2004) 3091–3095, https://doi.org/10.1016/j.electacta.2004.02.020.